

# MESOSCALE AND CONTINUUM CALCULATIONS OF WAVE PROFILES FOR SHOCK-LOADED GRANULAR CERAMICS

**T. J. Vogler<sup>1</sup> and J. P. Borg<sup>2</sup>**

<sup>1</sup>*Sandia National Laboratories, Albuquerque, New Mexico 87185-1181*

<sup>2</sup>*Marquette University, Milwaukee, Wisconsin 53233*

**Abstract:** Attenuating wave profiles from shock experiments on tungsten carbide powder are compared to calculations from the continuum P- $\lambda$  model and a 2-D mesoscale model to gain insight into the suitability of the two models. When calibrated, both models accurately capture the Hugoniot response of the powder and the arrival times of unattenuated steady waves. Their amplitudes are more accurately given by the mesoscale model since its reshock states are above the Hugoniot as seen experimentally; the P- $\lambda$  model, in contrast, reshocks along the Hugoniot. When the attenuating wave is in the range of the Hugoniot data, the models predict attenuation correctly. However, when attenuation falls below the Hugoniot data both models are somewhat inaccurate, and the material response seems to lie between the two models. The final aspect considered is the wave rise time, which is qualitatively correct for the mesoscale model but completely inaccurate for the P- $\lambda$  model.

**Keywords:** Granular materials, compaction, mesoscale modeling, wave attenuation, model validation

**PACS:** 62.50.+p.

## INTRODUCTION

Granular materials present modeling challenges due to their complex behavior under static and dynamic loading. Both simple continuum [1,2] and mesoscale [3,4] models have been used to describe their dynamic behavior. Regardless of the nature of the model, it is necessary to validate it against as wide a range of experimental data as possible in order to gain confidence in the model's performance. In this paper, we compare results of mesoscale and continuum simulations of the compaction of tungsten carbide (WC) powder to experimental data for attenuating shock waves. This comparison provides insight into the performance of the models and helps identify shortcomings in their behavior.

## EXPERIMENTAL DATA

Results for shock propagation in 56% dense WC powder have been reported [5]. The stepped target made from PMMA shown in Fig. 1 was filled with WC powder and then covered with a 1 mm thick aluminum plate. The steps create powder layers with nominal thicknesses of 1, 2.5, 4, 5.5, and 7 mm. A velocity interferometer (VISAR) was used to monitor the interface between the small aluminum disk on each level and a LiF window behind it. The aluminum cover plate was then impacted with a 12.7 mm thick plate of aluminum at nominal velocities of 245, 500, and 711 m/s. For the thinnest two or three layers of powder, steady structured waves were observed; for thicker layers the waves were attenuated by release waves from the back of the impactor. The steady waves were used to determine Hugoniot and reshock states [5]; here, we focus on the attenuated waves.

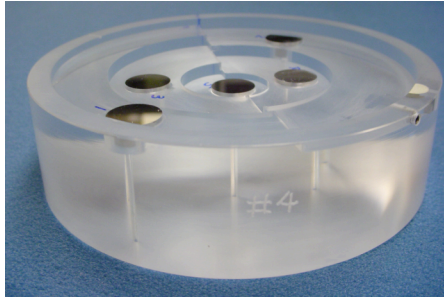


**Figure 1** Picture of fixture for experiments prior to filling showing the five steps and aluminum buffer plates.

## MODELS

Simulations using two models were performed using the hydrocode CTH. All components of the experiments (impactor, cover plate, powder, buffer, and window) are included in the simulations with nominal thicknesses, but edge release is not included. The first model is the continuum P- $\lambda$  model [2], a compaction model outlined elsewhere in this volume [6] that generalizes the P- $\alpha$  model [1]. As can be seen in Fig. 2, the calibrated P- $\lambda$  model agrees well with the shock data. Simulations were not performed with P- $\alpha$  because the functional form for compaction implemented in CTH is poorly suited for granular ceramics [6]. In addition to initial density  $\rho_{oo}$ , two parameters are important:  $P_c$  and  $n$ .  $P_c$  describes the pressure at which compaction occurs, while  $n$  characterizes the range of pressure over which it occurs. Material parameters used in the simulations are given in Table 1. Although an elastic regime can be included in the model, we have used it in the hydrodynamic mode since it gave better agreement with the wave profiles.

The second model is a 2-D mesoscale model [3], also run within CTH, in which individual WC particles are idealized as circles (rods) as shown in Fig. 3. Simple Mie-Grüneisen EOS's are used for aluminum, LiF, and WC. An elastic-perfectly

Table 1 Values of parameters for P- $\lambda$  model.

$\rho_{oo}$	$P_c$	$n$
8.79 g/cm <sup>3</sup>	1.6 GPa	0.44

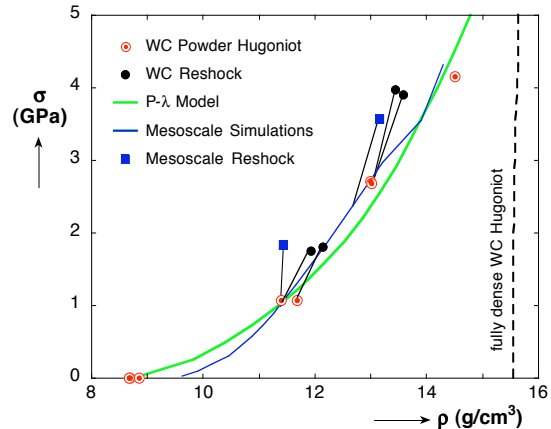


**Figure 2** Hugoniot responses from experiments, P- $\lambda$  model, and mesoscale simulations, along with reshock states.

plastic constitutive model is used for the WC particles, a Johnson-Cook plasticity model is used for aluminum, and LiF is assumed to behave hydrodynamically. Model parameters were taken from the literature and have been given previously [3]. Here, though, we increase the yield strength of WC from the 5 GPa used previously to 8 GPa so that the shock response of the model matches the experimental data as shown in Fig. 2. Also shown in the figure are reshock states from the experiments and the mesoscale simulations. Reshock states for the P- $\lambda$  model are not shown since they lie along the Hugoniot.



**Figure 3** Setup for the mesoscale model. Periodic boundary conditions used on top and bottom.

## RESULTS

Results from the P- $\lambda$  and mesoscale models are compared with those from an experiment at 500 m/s (WC-III in [5]) in Fig. 4. The experimental velocity records are cut off after a relatively short time because edge release in the small LiF windows (6 mm diameter) will result in deviations from uniaxial strain at longer times. Three thicknesses

display unattenuated waves. Arrival times for these agree well for both models as expected since the shock velocity (with impedance matching to the cover plate) determines the Hugoniot state. However, the velocity amplitudes of the mesoscale model match those from experiments better than the P- $\lambda$  model. This appears to be due to differences in reshock behavior between P- $\lambda$ , which reshocks along the Hugoniot, and the mesoscale model, which reshocks above it as can be seen in Fig. 2. Waves in the two remaining thicknesses are attenuated to about 60% and 50% of the steady wave amplitude. The arrival times and amplitudes of the waves are predicted about equally well by the two models.

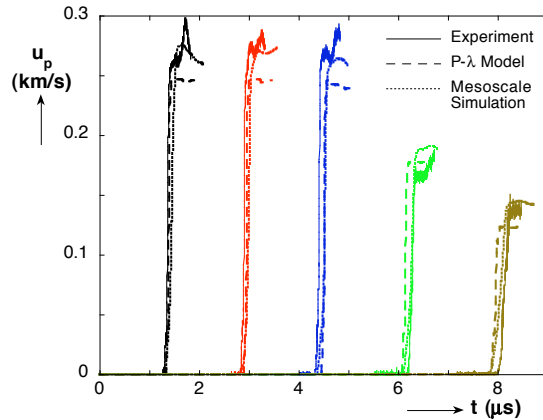


**Figure 4** Measured and predicted window velocity histories for five sample thicknesses for an experiment at 500 m/s.

Experimental and model results for an experiment at 245 m/s (WC-I in [5]) are shown in Fig. 5. Here, only two of the thicknesses display unattenuated waves. The arrival times of these waves are predicted well by both models, but their amplitude is captured better by the mesoscale model. Again, this is due to the stiffer reshock of the experiments and the mesoscale model. The remaining three waves are attenuated to about 65, 45, and 35% of the steady amplitude. In all three cases, the waves from the mesoscale simulations arrive slightly later than in the experiments, while those for P- $\lambda$  arrive somewhat earlier. The amplitudes of the attenuated waves are predicted more accurately by P- $\lambda$  than by the mesoscale

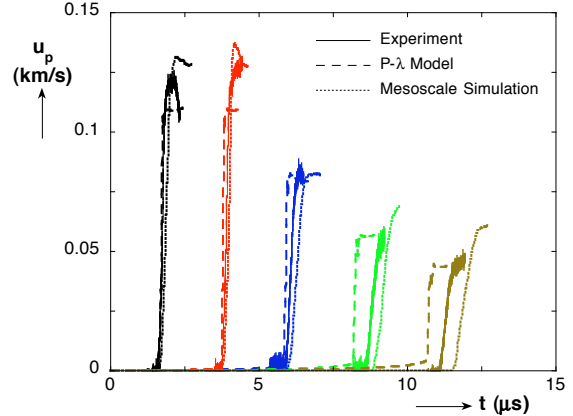


**Figure 5** Measured and predicted window velocity histories for five sample thicknesses for an experiment at 245 m/s.

model, which somewhat overpredicts the amplitude of the fourth and fifth waves.

To allow the wave shapes to be examined in detail, the velocity histories from Fig. 5 (245 m/s) are shown shifted in time so that they overlap one another in Fig. 6. The steadiness of the first two waves is evident in the experiment and for P- $\lambda$ , but the wave amplitudes and shapes are somewhat different for the mesoscale model. This difference appears to arise from temporal and spatial variations in the wave as it propagates through the mesoscale model (cf. Figs. 7 and 10 of [3]).

As the wave attenuates in the experiment, it spreads out due to the dispersive nature of the granular material. The mesoscale profiles are very

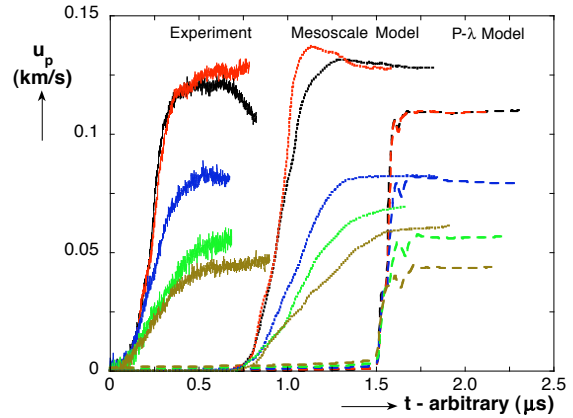


**Figure 6** Time-shifted window velocity histories for a 245 m/s experiment.

similar to the experimental ones in this regard, but those from P- $\lambda$  have nearly the same rise time regardless of their amplitude. Previous work [5,6] has shown a nearly linear scaling between strain rate and stress for steady waves in granular ceramics; a similar scaling was found for the mesoscale model [3]. When the rise times of the waves are plotted against their amplitudes in Fig. 7, one can see that the behavior is very similar in the model and the experiment, though the rise times are slightly longer for the model. Also, steady waves at 245 m/s have similar rise times to the attenuated waves from 500 m/s. Thus, the rise time appears to be primarily controlled by the wave amplitude with only a modest dependence on its history.

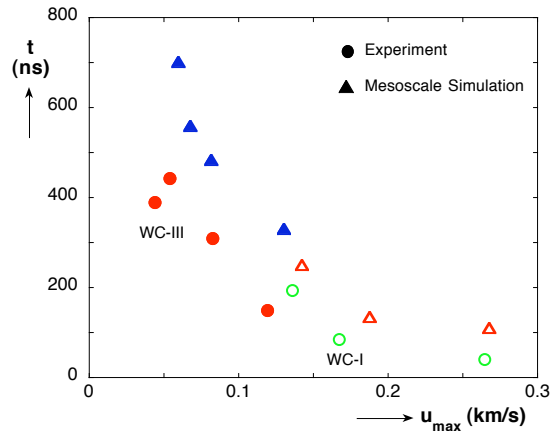


**Figure 7** Wave rise times from mesoscale simulations and experiments as a function of particle velocity amplitude of the wave.

## DISCUSSION AND CONCLUSIONS

In this paper, we have examined wave profiles for WC powder as a means to discriminate the suitability of different computational models for granular ceramics. While both the continuum P- $\lambda$  and mesoscale models capture the Hugoniot states well, the experimental reshock states lie above the Hugoniot, a feature captured by the mesoscale model but not the P- $\lambda$  model. This appears to be due to the formation of new microstructures during the shock process that stiffen the material.

Both models correctly capture the attenuation of the wave in the 500 m/s experiment, but both are somewhat inaccurate for the 245 m/s one. For that

case, the P- $\lambda$  model is overly stiff, while the mesoscale model is somewhat soft. As the wave attenuates in the 500 m/s case, it still is about the same amplitude as the 245 m/s steady waves. Thus, the attenuating wave for the former case is within the stress range for which the model has been calibrated, while in the latter case the attenuating wave is at stresses below the available Hugoniot data. In fact, attenuating waves appear to be a viable means to probe the response at very low stresses that might otherwise be inaccessible, and the response of the powder in that regime seems to lie between the P- $\lambda$  and mesoscale models.

Waves predicted by the two models differ significantly in their rise times. While waves in the mesoscale model are spread out as in the experiment, those from the P- $\lambda$  show quite short rise times that do not vary significantly with amplitude. This could be important in applications where granular materials are used for shock mitigation as a dispersive wave is less likely to lead to spall or explosive initiation.

## ACKNOWLEDGEMENTS

Sandia is a multi-program laboratory operated by Sandia Corporation, a Lockheed Martin Company, for the United States Department of Energy under Contract DE-AC04-94AL85000.

## REFERENCES

1. W. Herrmann, *J. Appl. Phys.* **40**, 2490 (1969).
2. D.E. Grady et al., *J. Phys. IV* **10**, 15 (2000); D.E. Grady and N.A. Winfree, in *Fundamental Issues and Applications of Shock-Wave and High-Strain-Rate Phenomena* (Elsevier, New York, 2001), pp. 485-491.
3. J.P. Borg and T.J. Vogler, *Int. J. Solids Structures* (submitted) (2007).
4. D.J. Benson, in *High-Pressure Shock Compression of Solids IV: Response of Highly Porous Solids to Shock Loading* (Springer-Verlag, N.Y., 1997), pp. 233-255.
5. T.J. Vogler, M.Y. Lee, and D.E. Grady, *Int. J. Solids Structures* **44**, 636 (2007).
6. J.A. Brown et al., in *Shock Compression of Condensed Matter-2007* (AIP, New York, 2008) this volume.